Polymer Chemistry

Accepted Manuscript

This article can be cited before page numbers have been issued, to do this please use: R. Chiarcos, L. Gabutti, E. Marsengo, D. Antonioli, M. Perego and M. Laus, *Polym. Chem.*, 2026, DOI: 10.1039/D5PY01210D.

ROYAL SOCIETY OF CHEMISTRY

rsc.li/polymers

Degrafting reaction of polymer brushes: the determining role of molecular weight and grafting density

Riccardo Chiarcos[a], Diego Antonioli[a], Luca Gabutti[a], Elo Marsengo[a], Michele Perego[b] and Michele Laus[a]

[a]Department of Science and Technological Innovation (DISIT), Università del Piemonte Orientale (UPO), Alessandria 15121, Italy
[b]Institute for Microelectronics and Microsystems (IMM), National Research Council of Italy (CNR), Agrate Brianza 20864, Italy

riccardo.chiarcos@uniupo.it

The chemical stability of polymer brushes is mandatory to ensure their applicability in a wide range of environments. However, it is well-known that, in presence of water, polymer chains detach from the substrate due to the hydrolytic cleavage of the anchoring bonds at the polymer-substrate interface. Furthermore, this degrafting reaction is promoted by the tension generated on the labile anchoring bonds by the swelling of the brush. It is now widely demonstrated that the brush tension increases, speeding up the degrafting reaction, as the number of chains per unit of area (grafting density) increases. On the contrary, the role of the molecular weight of the grafted polymer on the degrafting reaction is much less investigated. In this work, polymer brushes made up of polystyrenes with different molecular weights were obtained by the grafting to approach. Chain degrafting was then induced by a THF/water mixture and the progress of the degrafting reaction was followed by thickness measurements on the dry brushes. The reaction rate constant of the degrafting process was calculated as a function of both the grafting density and the molecular weight of the polymer, confirming that both parameters have a significant role. Furthermore, the degrafting reaction was also evaluated in brushes containing long and short chains in different percentages. A reciprocal influence was observed between the two components, with the overall degrafting process being precisely dictated by the majority one.

Introduction.

Adaptable and programmable surfaces are highly requested in all those applications in which the interaction between a material and the surrounding enviroment is critical[1]. Among the tools of surface engineering, polymer brush technology is certainly the most promising[2, 3, 4]. In fact, polymer brushes, which consist of polymer chains chemically anchored by one end to a substrate, are currently evaluated for a broad range of applications such as sensing[5, 6, 7], electronics[8, 9, 10, 11, 12], membranes[13, 14], adhesives[15, 16], energy devices[17], lubricants[18, 19, 20, 21], biocompatible coatings[22, 23] and bioscience[3, 24, 25, 26].

Polymer brushes are generally obtained through two distinct approaches, grafting from and grafting to [4, 27]. In grafting from, the substrate is initially reacted with functional initiator and then the polymer chains are grown from the substrate dipped in a monomer solution[28]. Although several polymerization techniques are suitable for the grafting from approach, the most common is undoubtedly the Surface Initiated-Atom Transfer Radical Polymerization (SI-ATRP), which allows several monomers to be polymerized and leads to polymers with controlled molecular weights and relatively narrow weight distributions[29, 30, 31, 32, 33, 34]. The grafting from approach is certainly the most suited for the synthesis of brushes with high grafting densities (Σ, number of chains for unit of area) and thicknesses (H). However, the need to detach the grafted chains, also taking into account their very low amount, makes not-trivial their characterization. Conversely, in the grafting to process polymers with functional end-groups are synthesized, fully characterized and then chemically attached to the substrate[35]. The drawback of this approach is the limited grafting density that can be achieved due to the self-limiting nature of the grafting to reaction[36]. In fact, it has been widely demonstrated that the maximum

View Article Online
DOI: 10.1039/D5PY01210D

obtainable values of both H and Σ of a brush obtained by grafting to depend on the molecular weight of the grafted polymer[37, 38, 39, 40, 41]. Interestingly, this relation between the maximum grafting density achievable and the molecular weight of the polymer was recently exploited for silicon doping applications in microelectronics[12, 42, 43].

If grafting reactions are the tools that enable brush synthesis, the reverse process, generally called degrafting, deserves no less attention[27]. For example, the self-limiting nature of the grafting to process was recently reconsidered evaluating the competitive role of the degrafting reaction, that brings the system to a dynamic equilibrium condition[44, 45, 46]. However, most of the attention addressed to the degrafting process is focused on evaluating the stability of polymer brushes, eventually in application environment[27, 47, 48]. In particular, it was highlighted that the presence of water plays a decisive role in the detachment of the brush by breaking the hydrolysable bonds between polymers and substrate[27, 49]. When silicon oxide is used as the substrate, most common case, the hydrolysis reaction occurs on both siloxane and ester/amide bonds that are typically contained in the linker between the polymer and the substrate[50, 51, 52]. Moreover, since Si-O bonds are the anchoring points of the SI-ATRP initiators on the substrate, improved brush stability was achieved by replacing them with non-hydrolyzable Si-C bonds[51, 53]. Hydrolysable linkages of Si-O type are also obtained in present in brushes prepared by grafting to reactions of hydroxy-terminated polymers to silicon oxide[44, 46].

Although hydrolysis resistance of the brush remains challenging, the use of hydrophobic SI-ATRP initiators or the inclusion of protective hydrophobic polymer blocks can markedly reduce the water access to the hydrolysable groups and, consequently, the degrafting process[54, 55].

While degrafting reactions were recently observed also for brushes in humid environments[56, 57], polymer detachment takes place principally when polymer brushes are exposed to water containing solvents[27]. In this conditions, the brush tends to absorb the solvent for osmosis, thus swelling and stretching the polymer chains perpendicularly to the substrate[58]. Furthermore, the chain stretching produces a tension (f) on the chain anchoring point that was estimated as [59, 60, 61]

$$f \propto \frac{k_B T}{\xi} = k_B T \Sigma^{0.5} \qquad \text{Eq. 1}$$

where k_B is the Boltzmann constant, T is the temperature, ξ is the distance between two neighbouring grafting sites and Σ is the grafting density of the brush. The relation between ξ and Σ is commonly considered to be $\xi = \Sigma^{-0.5}$ [62]. **Equation 1** indicates that when the grafting density increases the polymer chains are more crowded and stretched thus increasing the tension at the interface. The force f, also for the highest Σ values achievable in polymer brushes, does not exceed few pN and thus it is not sufficient to produce a direct bond break, for which several nN are required[34]. However, it was recently demonstrated that f is generally strong enough to catalyse other reactions involving the anchoring bond of polymer brushes, in particular hydrolysis, thus leading to degrafting processes[27, 34, 63]. There are several examples in literature reporting degrafting reactions in which polymer detachment is faster at higher Σ and thus slower as Σ decreases[50, 52, 63, 64]. This effect makes degrafting reactions complex processes in which the reactivity (and thus the reaction rate constant k) strongly depends on the chain environment in the brush.

Beyond the grafting density, also the affinity between polymer and solvent plays a crucial role in determining the brush degrafting tendency[63]. For example, Wang et al. treated poly(tert-butyl methacrylate) brushes with different organic solvents containing a defined amount of water and observed that the degrafting kinetic constant k increases in parallel with the polymer swelling ratio, which becomes more pronounced the more affine the solvent is[63]. The more affine the solvents are for the brush, the greater the quantity that enters the brush, thus increasing the chain stretching and, consequently, the tension f at the interface. Furthermore, for polyelectrolyte brushes in aqueous solutions both pH and salts can influence the brush swelling and consequently the degrafting kinetics[47, 48, 50, 52, 54, 65]. Therefore, the same brush can result stable or not in different environments.

View Article Online
DOI: 10.1039/D5PY01210D

A further parameter that seems to influence the brush degrafting is the molecular weight of the grafted polymer[50]. Although the polymer molecular weight doesn't appear to be a relevant parameter in determining f, according to **Equation 1**, there is a fair amount of evidence that brushes consisting of long polymer chains are keen to degraft faster than brushes made of short chains[48, 50, 54, 64]. In contrast, there is also a limited number of studies reporting slight or no influence of the molecular weight on k[52, 63]. In this context, a systematic study was performed by Melzak et al.[64] to evaluate the degrafting of poly(N,N-dimethylacrylamide) brushes with different molecular weight and grafting density in methanol solutions. In this study, a clear dependence of the degrafting rate constant on the molecular weight was observed with the higher molecular weight brushes undergoing the degrafting faster than the lower molecular weight brushes. However, the interpretation of some experimental results in that paper is inconsistent. In particular, the degrafting of the polymer with the highest molecular weight ($3.63*10^5$ g/mol) presents a marked decrease of k from 1.27 to 0.024 min^{-1} when Σ decreases from 0.79 to 0.31 chains/nm^2. This decrease was attributed to reduced interactions between vicinal grafted chains and, consequently, to a reduced tension at the anchoring points. However, when the degrafting of fresh brushes with the same molecular weight but initial Σ of 0.11 chains/nm^2 was evaluated, a k value of 0.41 min^{-1} was calculated. This value is much higher than 0.024 min^{-1} obtained in the first experiment for Σ lower than 0.31 chains/nm^2. Furthermore, the Σ level beyond which the interaction between vicinal chains reduces results higher for the polymer with a molecular weight of $3.63*10^5$ g/mol than to smaller polymers with molecular weights of $7*10^4$ and $4.3*10^4$ g/mol. This finding is unreasonable, as the volume occupied by a polymer increases with the molecular weight. These unsolved points, in combination with the incompleteness of the theory leading to **Equation 1**, makes necessary further investigations of the molecular weight effect on the degrafting reaction of polymer brushes. Furthermore, a comprehensive study of degrafting in widely disperse systems containing polymers with different molecular weights is still lacking, despite their common use in applications.

In the present work, the degrafting of polystyrene brushes obtained by grafting to was investigated in a tetrahydrofuran (THF) solution containing water. The use of polystyrene as a model polymer is motivated by the fact that it does not contain neither cleavable nor ionisable groups in the main chain, which would add further variables to the study of the degrafting process. The clarification of the roles of both the molecular weight and the grafting density on the degrafting rate constant was the main focus of this work and the influence of these parameters were evaluated during the entire degrafting process. Furthermore, bimodal brushes containing different amounts of short and long polymers were also investigated with the aim to evaluate degrafting in dispersed systems. The degrafting rate constant of the short and the long component of the brush were determined and evaluated as a function of the brush composition.

Results and discussion.

A hydroxy-terminated deuterated polystyrene with number average molecular weight (M_n) of 5.2 kg/mol (dispersity index Đ = 1.12) and two hydroxy-terminated hydrogenated polystyrenes with M_n of 13 kg/mol (Đ = 1.06) and 43.2 kg/mol (Đ = 1.16) were synthesized by ARGET-ATRP (Activator ReGenerated by Electron Transfer-Atom Transfer Radical Polymerization) technique[41, 42, 66]. More details on the synthesis and characterization are published elsewhere[45]. The three samples are indicated as PS_{d8}5.2-OH, PS13-OH and PS43.2-OH respectively.

Degrafting reaction in single polymer brushes. Polymer brushes consisting of one between PS_{d8}5.2-OH, PS13-OH or PS43.2-OH were obtained by the grafting to approach on silicon wafer substrates covered by a ~ 2nm thick layer of native oxide (SiO_2). The scheme of the reaction is represented in **Figure 1** and consists of a condensation between the hydroxyl end-group of the polystyrene and the surface silanols[46]. In details, a thin layer (30 nm) of the functional polymer was deposited by spin-coating on the substrate and the grafting to reaction was performed at 250 °C for 900 s in melt conditions under inert atmosphere. The reaction conditions were selected to achieve the maximum

View Article Online
DOI: 10.1039/D5PY01210D

values of H and Σ, in accordance with the self-limiting nature of the process[45, 46]. The unreacted chains were removed by toluene washes and the thickness of the dry brush was evaluated by ellipsometry. A representation of the overall process is included in the Supporting Information (see **Figure S1**). The average thickness of the obtained brushes (H_0) was 4.3, 7.6 and 14.5 nm when PS_{d8}5.2-OH, PS13-OH and PS43.2-OH were used, respectively. The grafting densities of the brushes were also calculated by **Equation 2**[67],

$$\Sigma = \frac{HdN_A}{M_n} \qquad \text{Eq. 2}$$

where H is the brush thickness, d the polymer density, N_A the Avogadro's number and M_n the average molecular weight of the grafted polymer. The average grafting densities (Σ_0) were 0.52, 0.37 and 0.21 chains/nm^2 for PS_{d8}5.2-OH, PS13-OH and PS43.2-OH brushes, respectively. Both H_0 and Σ_0 values are in good accordance with literature[45].

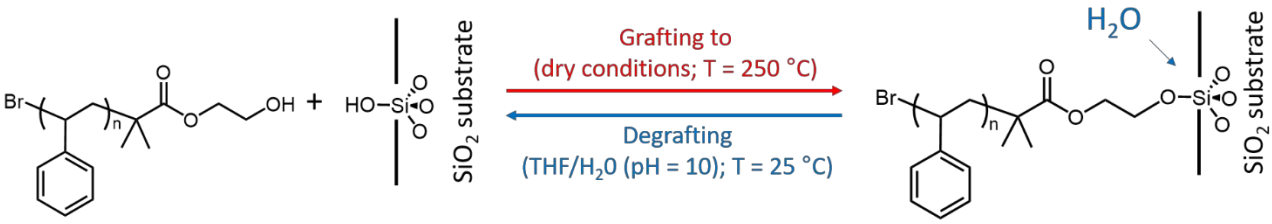

Figure 1. Grafting to and degrafting reactions of hydroxy-terminated polystyrenes on SiO_2 substrates.

The degrafting reaction was performed at room temperature by immersing the polymer brushes in a mixture consisting of 75% THF and 25% of a pH = 10 buffer solution. This mixture turned out to be much more effective than either simple deionized water or pH = 10 buffer solution alone, as clearly appears in **Figure S2**. The addition of THF makes the mixture significantly more affine to polystyrene, thus promoting the swelling of the brush and the access of the mixture at the polymer/substrate interface. Consistent with this, THF and water mixtures with similar percentages were already used for study degrafting reactions[63]. In the present work, a pH = 10 buffer solution was used instead of pure water to speed up the reaction. The expected reaction is essentially the reverse of the grafting to reaction (see **Figure 1**) and consists in the hydrolysis of the siloxane bond anchoring the polymer at the substrate.

The hydrolysis of the polymer chains from the brush layer was monitored by recording the thickness of the dried brush after different times of exposure to the degrafting solution. The obtained H values are reported in **Figure 2 (a)**. Similarly, the relative Σ values were calculated by **Equation 2** and are reported in **Figure 2 (b)**. Obviously, H and Σ present similar trends with a steep initial decrease followed by a slower decrease for long times.

View Article Online
DOI: 10.1039/D5PY01210D

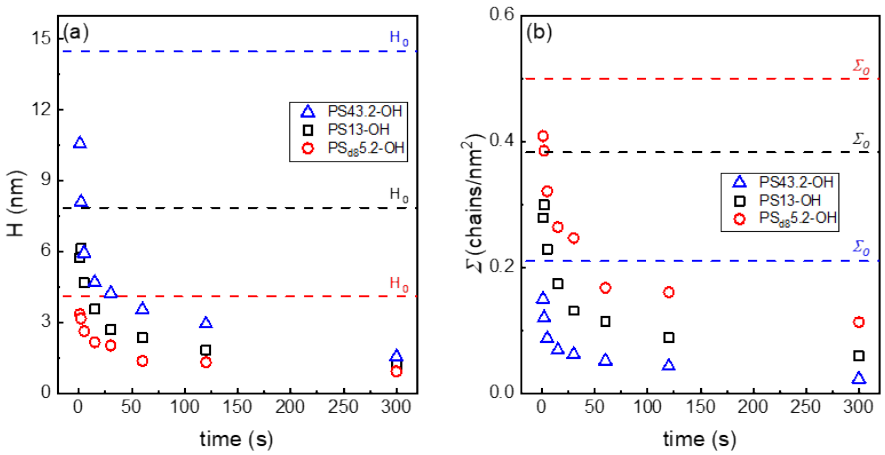

Figure 2. H **(a)** and Σ **(b)** values as a function of the degrafting time for the polymer brushes consisting of PS_{d8}5.2-OH (red dots), PS13-OH (black dots) and PS43.2-OH (blue dots). The values of H_0 and Σ_0, relative to the brushes before degrafting, are also included as dotted lines.

It was already argued that the hydrolysis-degrafting reactions can be reasonably described by pseudo-first order kinetics, assuming that water is constant throughout the entire course of the reaction[65]. In this perspective approach, the reaction rate constant (k) is estimated as the slope of the curve obtained by plotting $\ln(\Sigma/\Sigma_0)$ as a function of the degrafting time, as reported in **Figure 3 (a)**. The most immediate evidence is that the slope of the degrafting curve is not constant but decreases as the reaction proceeds, thus leading to a parallel decrease of k. This phenomenon was already described in literature[54], [64] and is promoted by the tension f that the swollen and stretched chains induce on the anchoring points[34]. Therefore, since f decreases as Σ decreases, as indicated in **Equation 1**, k is expected to decrease as the degrafting proceeds.

The value of k at each degrafting time was obtained by fitting the data reported in **Figure 3 (a)** and making the derivative of the obtained curve. Furthermore, to have a direct relation between k and Σ during the reaction course, at each degrafting time was assigned the corresponding grafting density by fitting the data reported in **Figure 2 (b)**. Finally, the values of k and Σ corresponding to the same degrafting time were associated, obtaining the curves reported in **Figure 3 (b)**. More details on the fitting method are reported in the Supporting Information. The dependence of k on Σ is confirmed across the entire grafting density range. In more detail, k decreases as Σ decreases steeply at first and then, once a critical value of Σ (Σ_c) is reached, more gradually, thus suggesting the presence of two different regimes in which the degrafting occurs.

Furthermore, for each value of Σ, k is systematically higher for the polymer with the higher M_n, thus confirming that the detachment from the substrate is faster the higher is the molecular weight. The difference of k for low and high molecular weight polymers is particularly evident for $\Sigma > \Sigma_c$, whereas the difference being less pronounced. Finally, the value of Σ_c depends on the molecular weight of the polymer, with Σ_c of PS_{d8}5.2-OH, PS13-OH and PS43.2-OH resulting approximately 0.27, 0.17 and 0.07 chains/nm^2, respectively.

View Article Online
DOI: 10.1039/D5PY01210D

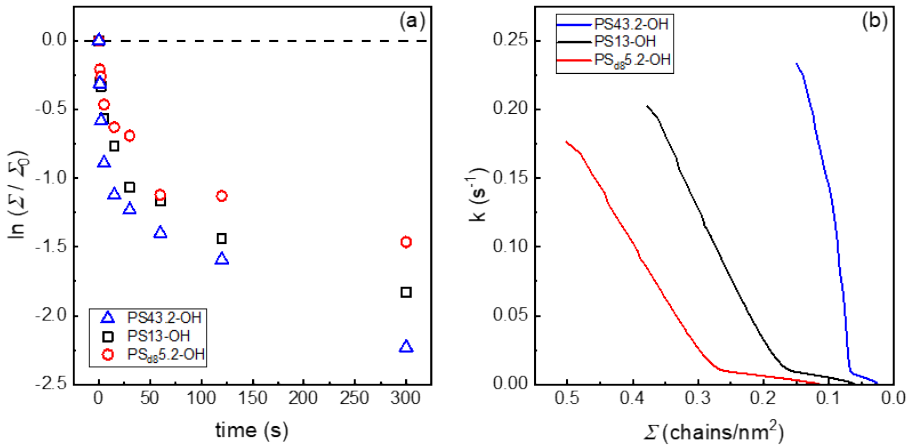

Figure 3. Ln(Σ/Σ_0) vs degrafting time **(a)** and k vs Σ **(b)** for the polymer brushes consisting of PS_{d8}5.2-OH (red), PS13-OH (black) and PS43.2-OH (blue).

A reasonable interpretation of the data presented in **Figure 3 (b)** is that for $\Sigma < \Sigma_c$ the grafted chains are far enough and do not significantly interact with each other. Consequently, there is a neglectable tension f at the anchoring points. On the contrary, for $\Sigma > \Sigma_c$, inter-chain interactions take place more strongly and generate the tension f which promotes the hydrolytic reaction thus resulting in an increase of k, as predicted by **Equation 1**. In this perspective, Σ_c is lower for the polymer with the higher molecular weight because of its larger volume, in good accordance with the experimental evidence. A first-order estimation of the grafting density at which the polymer chains begin to overlap is given by $1/\pi R_g^2$, where R_g represents the radius of gyration of the polymer within the brush and πR_g^2 is the area occupied by a single chain. As a first approximation, R_g can be calculated using **Equation 3**[45],

$$R_g = \left(\frac{N}{6}\right)^{1/2} b \qquad \text{Eq. 3}$$

where N is degree of polymerization and b is the statistical segment length (0.68 nm for polystyrene[45]). The three samples PS_{d8}5.2-OH, PS13-OH and PS43.2-OH are characterized by R_g values of 1.89, 3.10 and 5.66 nm respectively, corresponding to overlap Σ of 0.09, 0.03 and 0.01 chains/nm^2. Notably, **Equation 3** estimates R_g of polymer in the melt state or in a theta-solvent, whereas in presence of a more compatible solvent R_g may increase leading to a subsequent decrease in the overlap Σ[36]. In all cases, the observed Σ_c values are systematically higher than the expected overlap threshold. This suggests that inter-chain interactions become significant in generating tension only when the polymer brush is already partially crowded.
In any case, it should be stressed that **Equation 1** is largely incomplete because it does not include a specific dependence of f to the molecular weight of the grafted polymer chain. Further research is certainly necessary to identify all the actors involved in the degrafting process. However, what is clear is that the role of M_n cannot be ignored when polymer brushes obtained with classical grafting to approaches are subjected to degrafting.
The following section will be dedicated to the study of degrafting in disperse brushes, where long and short polymers are grafted together.

Degrafting reaction in bimodal polymer brushes. Bimodal polymer brushes containing both PS_{d8}5.2-OH and PS13-OH were prepared by grafting to. In particular, three polymer brushes containing

View Article Online
DOI: 10.1039/D5PY01210D

PS_{d8}5.2-OH at the percentage of 90, 50 and 20 %, indicated as Brush90, Brush50 and Brush20, were the target brushes.

It well known that, during the grafting to reactions, polymers with lower molecular weights react preferentially with the substrate[68, 69, 70]. This leads to an enrichment of short chains in the brush compared to composition of the initial polymer mixture. In details, when a mixture of polymer 1 and polymer 2 is grafted, the ratio between the grafting densities of the two polymers results[36]

$$\frac{\Sigma_1}{\Sigma_2} = X\left(\frac{M_{n1}}{M_{n2}}\right)^{-0.5} \quad \text{Eq. 4}$$

where Σ_1 and Σ_2 are the grafting densities of polymer 1 and polymer 2 in the brush, X is the molar ratio between polymer 1 and polymer 2 in the initial polymer mixture, M_{n1} and M_{n2} are the average molecular weights of polymer 1 and polymer 2. According to **Equation 4**, if $M_{n1} < M_{n2}$, then $\Sigma_1/\Sigma_2 > X$ and an enrichment of the short polymer 1 takes place in the brush. In this work, **Equation 4** was applied in the reverse way to find the right value of X that is required to obtain a brush with a desired composition.

The grafting procedure was the same as described in the previous section. The thickness (H_0) of the brushes was determined by ellipsometry, while the brush composition was investigated by TGA-GC-MS (ThermoGravimetric Analysis-Gas Chromatography-Mass Spectrometry) analysis. The TGA-GC-MS procedure is now a consolidated approach for determining the composition of polymer brushes containing different polymer species[45, 71, 72, 73]. In this case, since the two components of the brush are polystyrenes differing in their M_n only, the contrast was produced by using a deuterated and a hydrogenated polystyrene sample. Briefly, in the TGA oven the brush was heated to promote the degradation of the polymers via an unzipping process, that generates principally monomers[71]. The monomers are conveyed in an inert gas flow, to a GC and analyzed in the mass detector. The intensity of the signals after proper calibration relative to deuterated styrene, for PS_{d8}5.2-OH, and hydrogenated styrene, for PS13-OH, were combined with the measurement of H_0 to give the grafting density of PS_{d8}5.2-OH ($\Sigma_{D,0}$), the grafting density of PS13-OH ($\Sigma_{H,0}$) and the total grafting density of the brush ($\Sigma_{TOT,0} = \Sigma_{D,0} + \Sigma_{H,0}$)[45]. More details on the measurements and calculations are contained in the Experimental Section. The characteristics of the obtained brushes are reported in **Table 1**.

Table 1. Target molar percentage of PS_{d8}5.2-OH, thickness (H_0), grafting density of the PS_{d8}5.2-OH component ($\Sigma_{D,0}$), grafting density of the PS13-OH component ($\Sigma_{H,0}$), total grafting density ($\Sigma_{TOT,0}$) and measured molar percentage of PS_{d8}5.2-OH of the grafted bimodal brushes.

Sample	% PS_{d8}5.2-OH target	H_0 (nm)	$\Sigma_{D,0}$ (chains/nm^2)	$\Sigma_{H,0}$ (chains/nm^2)	$\Sigma_{TOT,0}$ (chains/nm^2)	% PS_{d8}5.2-OH measured
Brush90/10	90	4.7	0.44	0.05	0.49	88
Brush50/50	50	6.1	0.24	0.20	0.44	54
Brush20/80	20	7.4	0.07	0.33	0.40	19

The degrafting procedure was the same as described in the previous section for single polymer brushes. The values of H measured after different degrafting times are reported in **Figure S6**. The composition of the brushes was also determined with TGA-GC-MS analysis and Σ_D, Σ_H and Σ_{TOT} are reported in **Figure 4**. Both the partial and the total grafting densities follow the same trend that was already reported for the single polymer brushes, with a rapid decrease at short degrafting times, followed by a slower decrease at longer times. The same behavior was observed for Brush90, Brush50 and Brush20.

View Article Online
DOI: 10.1039/D5PY01210D

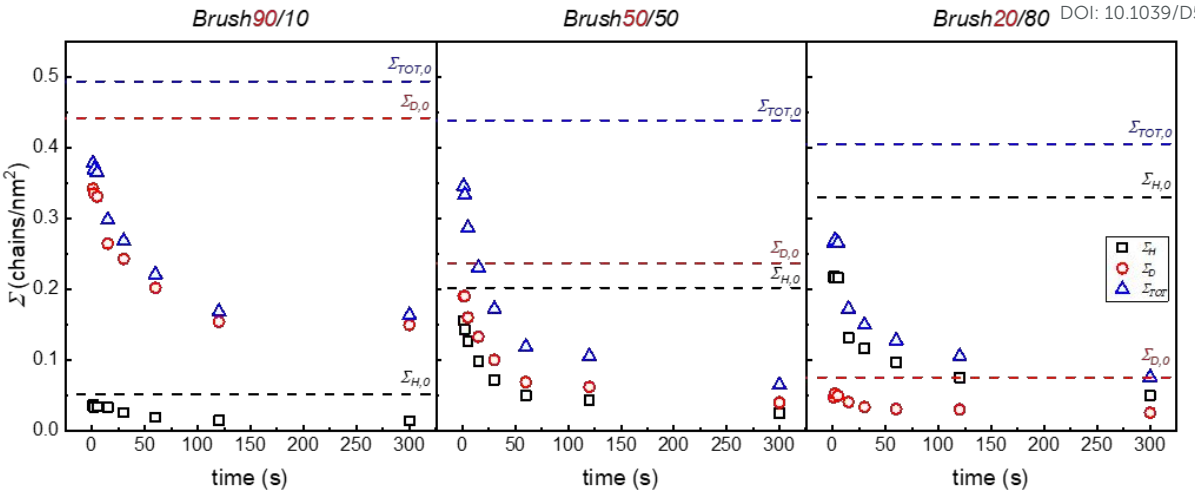

Figure 4. $\Sigma_{D,}$ Σ_H and Σ_{TOT} as a function of the degrafting time for the brushes Brush90, Brush50 and Brush20. The values of $\Sigma_{D,\,0,}$ $\Sigma_{H,\,0}$ and $\Sigma_{TOT,\,0}$, relative to the brushes before degrafting, are also included as dotted lines.

To further explore the degrafting kinetics, $\ln(\Sigma_D/\,\Sigma_{D,\,0})$ and $\ln(\Sigma_H/\,\Sigma_{H,\,0})$ were reported as a function of the degrafting time for each typology of brush (see **Figure S7-S9**). The degrafting rate constants of both the deuterated and hydrogenated component were then calculated as described in the previous section and reported in **Figure 5** as a function Σ_{TOT}. The presence of two regimes of degrafting is confirmed, even for disperse brushes. In fact, beyond a certain critical value of Σ_{TOT} ($\Sigma_{TOT,\,c}$) the dependence of k from Σ_{TOT} is definitely more marked than in the case in which Σ_{TOT} is lower than $\Sigma_{TOT,c}$. Interestingly, for each brush composition, $\Sigma_{TOT,\,c}$ of the two components has essentially the same value. Furthermore, the value $\Sigma_{TOT,\,c}$ decreases as the percentage of short chains (PS_{d8}5.2-OH) decreases from 90 to 20%. More in details, in the Brush90 the value of $\Sigma_{TOT,\,c}$ is approximately the same of Σ_c of the single PS_{d8}5.2-OH brush. In the same way, in the Brush20, $\Sigma_{TOT,\,c}$ and Σ_c of the single PS13-OH brush are similar. Finally, in the Brush50 the value of $\Sigma_{TOT,\,c}$ is between the Σ_c of the single PS_{d8}5.2-OH brush and the one of the single PS13-OH brush.
In general, the overall curves representing k vs Σ_{TOT} of both the components of the bimodal brushes are included between two limits, which consist of the curves obtained for the two single polymer brushes. More in details, the curves of the bimodal brush are shifted toward the limit-curve relative to the more abundant component of the brush. It is finally important to observe that, for $\Sigma_{TOT} > \Sigma_{TOT,c}$, k of PS13-OH is systematically higher than k of PS_{d8}5.2-OH, indicating a faster degrafting of the longest component of the brush. The preferential detachment of the longest components of disperse brushes is in good accordance with literature[64].

View Article Online
DOI: 10.1039/D5PY01210D

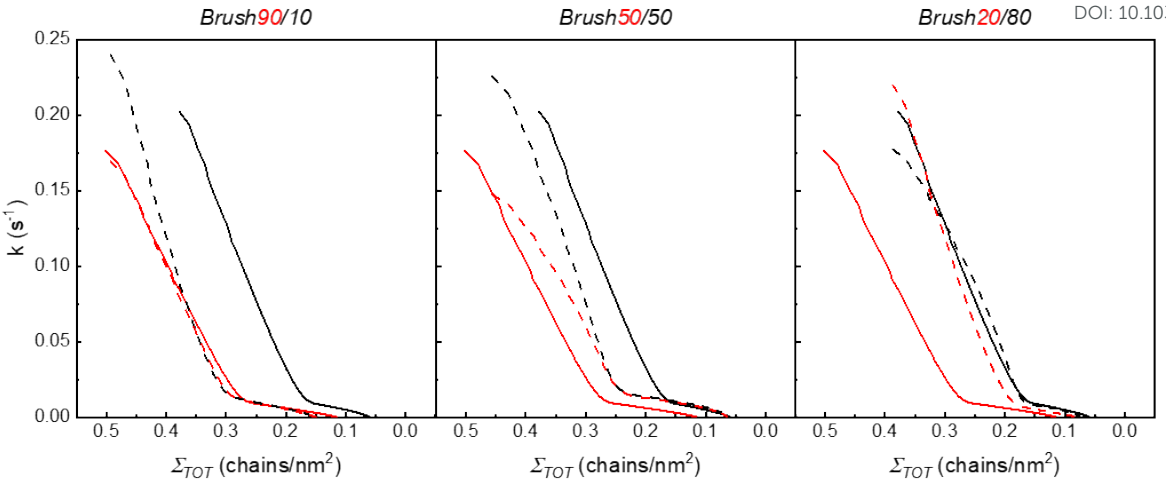

Figure 5. k vs Σ_{TOT} for the degrafting reaction of PS_{d8}5.2-OH (dotted red line) and PS13-OH (dotted black line) in the Brush90, Brush50 and Brush20. The curves representing k vs Σ for the degrafting reaction in the single polymer brushes (see **Figure 3 (b)**) are also included as references, with a full red line for PS_{d8}5.2-OH and a full black line for PS13-OH.

The main conclusion emerging from the data presented in **Figure 5** regards the presence of mutual interactions between short and long chains. For example, a single $\Sigma_{TOT,\,c}$ for of PS_{d8}5.2-OH and PS13-OH in each brush is observed. This means that the value of Σ_{TOT} at which the overall brush becomes tensioned is determined by mixed contacts between short and long polymers. Furthermore, for Brush20, the k of PS_{d8}5.2-OH increases up to the value typical of PS13-OH. On the other side, in Brush90 the k of PS13-OH decreases to the value typical of PS_{d8}5.2-OH. Therefore, in both cases, the minor component of the brush is forced by the interactions with the major components to assume a tension state typical of the latter thus indicating an interdependent dynamic.
The above evidences further confirm that the degree of tension, and consequently k, of a polymer in a brush is not only determined by the molecular weight and the grafting density, but also by the brush composition and dispersity with the overall degrafting kinetics complying with one of the major component.

Conclusions.

The degrafting reaction of polymer brushes constituted by two polystyrene samples with different molecular weights, and related blends with different compositions, was evaluated in a THF/water mixture. In all cases, a clear dependence of the degrafting rate constant on the grafting density of the brush was observed. In particular, the degrafting rate constant decreases linearly as the grafting density of the brush decreases with a sharp slope change corresponding to a critical grafting density value. For grafting densities lower than the critical value, the degrafting rate constant decreases slowly as the grafting density decreases. In contrast, when the grafting density is higher than the critical value, the degrafting rate constant decreases steeply. This behavior suggests the presence of two distinct regimes corresponding to tensioned and relaxed polymer chains in the brush. Furthermore, the critical grafting density value depends on the molecular weight of the polymer forming the brush. In addition, and contrary to theoretical prediction, in the range of grafting densities investigated, the degrafting of long polymer chains is faster than the degrafting of short ones. When brushes are prepared from blends of the two polystyrene samples with low and high molecular weight, the degrafting reaction of both components results similar to the one of the major species in the blend. This evidence suggests a mutual influence between the polymer chains in the brush, thus underscoring the cooperative nature of the degrafting mechanism. The overall picture provided by this work increases the understanding of the polymer brush stability, thus making it possible to produce adaptable surfaces able to change their structure and composition in a controlled way when applied

View Article Online
DOI: 10.1039/D5PY01210D

in specific environments. Furthermore, these data indicate the potential to create brush layers with customized responsiveness to external stimuli associated with specific environments, rendering them suitable for the fabrication of sensors to monitor detrimental environmental modifications and expanding the scope of applications for polymer brush layers.

Experimental Section.

Materials. The deuterated (PS_{d8}5.2-OH) and hydrogenated (PS13-OH) polystyrenes were synthesized by ARGET-ATRP using 2-hydroxyethyl-2-bromoisobutyrate (HEBIB) as the initiator to introduce a hydroxyl functionality in the polymer end-group. All the details of the synthesis and characterization were already published[45]. All the reagents were purchased by Merck and used as received. P-type Czochralski-grown Si(100) wafers (nominal resistivity of 1−5 Ω cm) were purchased from Siltronix.

PS43.2-OH synthesis and characterization. The sample was synthesized by a two-steps procedure. Firstly, a hydroxy-terminated polystyrene with M_n = 25.4 kg/mol (Đ = 1.12) was synthesized by ARGET-ATRP using 2-hydroxyethyl-2-bromoisobutyrate (HEBIB) as the initiator. More details of the synthesis and polymer characterization are reported in literature[42]. The molecular weight of this polymer was then increased by using it as a macroinitiator for a second ARGET-ATRP step[41]. In details, 1.5 g of the macroinitiator (59 µmol) was dissolved in a mixture consisting of 2 mL of styrene (monomer, 18 mmol, 300 equivalents), 526.3 µg of $CuBr_2$ (catalyst, 2.36 µmol, 0.04 equivalents), 0.6 µL of tris[2-(dimethylamino)ethyl]amine (ligand, 2.36 µmol, 0.04 equivalents) and 2 mL of anisole (solvent). The mixture was transferred in a Schlenk flask and degassed by two freeze-thaw cycles. After that, a solution consisting of 9.5 mg of Tin (II) 2-ethylhexanoate (reducing agent, 23.6 µmol, 0.4 equivalents), 6 µL of tris[2-(dimethylamino)ethyl]amine (ligand, 23.6 µmol, 0.4 equivalents) and 1 mL of anisole was added to the mixture and a further freeze-thaw cycle was performed. The reaction was carried out at 90 °C in a thermostatic oil bath for 17 h. The polymer was then purified by two successive precipitations carried out from a THF polymer solution in cold methanol. The M_n and Đ values of PS43.2-OH were determined by Size Exclusion Chromatography (SEC). The analysis was performed with a 590 Waters Chromatograph equipped with Waters HSPgel HR3 and HR4 columns and a refractive index detector. The eluent was THF, while the flow rate was 0.3 mL/min. The instrument was calibrated with polystyrene standards with molecular weights ranging from 1 to 100 kg/mol. The PS43.2-OH chromatograph is reported in **Figure S10**.

Grafting procedure. All the polymer brushes were obtained with the same procedure[68, 69]. Silicon wafers covered by a ~ 2 nm thick layer of native oxide were cut in slices of 1 cm x 1 cm, treated with piranha solution (H_2SO_4/H_2O_2 3/1 volume ratio) for 40 min at 80 °C, rinsed in deionized water and dried under nitrogen flow. The wafers were then washed with 2-propanol for 15 min in a sonication bath and dried with nitrogen flow. A ~ 30 nm thick layer of polymer were deposited on the wafer by spin-coating (3000 rpm, 30 s). The polymer solutions used for the spin-coating process are reported in **Table 2**.

Table 2. Composition of the solutions used in the spin-coating process. The amount of PS_{d8}5.2-OH, PS13-OH and toluene (solvent) for each typology of brush are reported.

Brush	PS_{d8}5.2-OH (mg)	PS13-OH (mg)	Toluene (mL)
Single PS_{d8}5.2-OH	9.0		1
Single PS13-OH		9.0	1
Brush90	6.2	2.8	1
Brush50	1.8	7.2	1
Brush20	0.5	8.5	1

The grafting to reaction of the deposited polymers were performed on a SAWATEC HP-150 hotplate located into a MBRAUN LABstar glovebox (inert atmosphere, H_2O, O_2 < 1 ppm). The reaction was carried out at 250 °C for 900 s. The unreacted chains were removed by toluene washes carried out in a sonication bath for 5 min. The wafers are finally dried under nitrogen flow.

View Article Online
DOI: 10.1039/D5PY01210D

Degrafting procedure. The sample was immersed in a mixture containing 75% THF and 25% Buffer solution pH = 10 (boric acid/potassium chloride/sodium hydroxide). The reaction was carried out at room temperature for different times. The samples were then rinsed in deionized water, dried under nitrogen flow, rinsed in fresh THF for 5 min and dried again under nitrogen flow.

Brush characterization. The brush thickness was measured with a FS-1 MultiWavelength Ellipsometer (Film Sense). The error of the measurement was seen to be less than 0.1 nm.

The composition of the bimodal brush was evaluated by TGA-GC-MS analysis. The TGA instrument was a Mettler Toledo TGA/DSC 3+ model, while the GC-MS apparatus was a Finnigan GC Trace 1300 MS ISQ LT instrument equipped with a Phenomenex DB5-5MS capillary column of 30 m of length, 0.25 mm of the inner diameter and 0.25 μm of thickness. The sample was annealed in the TGA oven from 25 to 1000 °C with a heating ramp of 20 °C/min under a helium flow (50 mL/min). The degradation products were collected and introduced in the GC-MS instrument. The signals revealed in the MS were acquired in EI+ mode in the Selected Ion Monitoring (SIM) mode, with specific focus on the species with m/z of 104 and 112, relative to styrene and deuterated styrene monomers respectively. More details on this hyphenated technique, including the temperatures of the transfer lines and the various segments, are published elsewhere[71, 73].

The areas of the signals relative to the species with m/z of 104 and 112, indicated as A_{STY} and A_{STYd8}, were demonstrated to be proportional to the molar amount of styrene and deuterated styrene in the analyzed brush[45]. The mass fraction of styrene ($F_{PS13\text{-}OH}$) in the brush is then calculated with **Equation 5**[45].

$$F_{PS13-OH} = \frac{A_{STY}104}{A_{STY}104 + A_{STYd8}112} \quad \text{Eq. 5}$$

Finally, the grafting density of the deuterated PS_{d8}5.2-OH polymer (Σ_D), of the hydrogenated PS13-OH polymer (Σ_H) and the total grafting density (Σ_{TOT}) were calculated with the following equations[45]:

$$\Sigma_D = \frac{(1 - F_{PS13-OH})HdN_A}{5200} \quad \text{Eq. 6}$$

$$\Sigma_H = \frac{F_{PS13-OH}HdN_A}{13000} \quad \text{Eq. 7}$$

$$\Sigma_{TOT} = \Sigma_D + \Sigma_H \quad \text{Eq. 8}$$

Conflicts of interests.

There are no conflicts to declare.

Acknowledgements. We acknowledge Professor Giuseppe Milano for the fruitful exchanges of opinions that took place during the research work and the analysis of the data.

References.

1 A. S. Goldmann, N. R. B. Boase, L. Michalek, J. P. Blinco, A. Welle and C. Barner-Kowollik, *Adv. Mater.*, 2019, **31**, 1–21.

2 S. V. Orski, K. H. Fries, S. K. Sontag and J. Locklin, *J. Mater. Chem.*, 2011, **21**, 14135–14149.

3 W. L. Chen, R. Cordero, H. Tran and C. K. Ober, *Macromolecules*, 2017, **50**, 4089–4113.

4 W. J. Brittain and S. Minko, *J. Polym. Sci., Part A Polym. Chem.*, 2007, **45**, 3505–3512.
5 H. Liu, Y. Li, K. Sun, J. Fan, P. Zhang, J. Meng, S. Wang and L. Jiang, *J. Am. Chem. Soc.*, 2013, **135**, 7603–7609.
6 N. Fortin and H. Klok, *ACS Appl. Mater. Interfaces*, 2015, **7**, 4631–4640.
7 L. A. Smook, G. C. Ritsema van Eck and S. de Beer, *ACS Appl. Polym. Mater.*, 2021, **3**, 2336–2340.
8 E. Han, K. O. Stuen, M. Leolukman, C. C. Liu, P. F. Nealey and P. Gopalan, *Macromolecules*, 2009, **42**, 4896–4901.
9 F. Ferrarese Lupi, T. J. Giammaria, F. G. Volpe, F. Lotto, G. Seguini, B. Pivac, M. Laus and M. Perego, *ACS Appl. Mater. Interfaces*, 2014, **6**, 21389–21396.
10 S. Wang, Z. Wang, J. Li, L. Li and W. Hu, *Mater. Chem. Front.*, 2020, **4**, 692–714.
11 S. Wang, Z. Wang, Y. Huang, Y. Hu, L. Yuan, S. Guo, L. Zheng, M. Chen, C. Yang, Y. Zheng, J. Qi, L. Yu, H. Li, W. Wang, D. Ji, X. Chen, J. Li, L. Li and W. Hu, *ACS Appl. Mater. Interfaces*, 2021, **13**, 17852–17860.
12 R. Chiarcos, M. Laus and M. Perego, *Eur. Polym. J.*, 2024, **208**, 112849.
13 J. J. Keating IV, J. Imbrogno and G. Belfort, *ACS Appl. Mater. Interfaces*, 2016, **8**, 28383–28399.
14 E. Nur Durmaz, S. Sahin, E. Virga, S. de Beer, L. C. P. M. de Smet and W. M. de Vos, *ACS Appl. Polym. Mater.*, 2021, **3**, 4347–4374.
15 K. B. Buhl, A. H. Agergaard, M. Lillethorup, J. P. Nikolajsen, S. U. Pedersen and K. Daasbjerg, *Polymers*, 2020, **12**, 1475.
16 Y. Yu, M. B. Pérez, C. Cao and S. de Beer, *Eur. Polym. J.*, 2021, **147**, 110298.
17 J. M. Giussi, M. Lorena Cortez, W. A. Marmisolle and O. Azzaroni, *Chem. Soc. Rev.*, 2019, **48**, 814–849.
18 T. Kreer, *Soft Matter*, 2016, **12**, 3479–3501.
19 J. Klein, E. Kumacheva, D. Mahalu, D. Perahla and L. J. Fetterst, *Nature*, 1994, **370**, 634–636.
20 S. De Beer, E. Kutnyanszky, P. M. Schon, G. J. Vancso and M. H. Muser, *Nat. Commun.*, 2014, **5**, 3781.
21 W. Yan, S. N. Ramakrishna, N. D. Spencer and E. M. Benetti, *Langmuir*, 2019, **35**, 11255–11264.
22 K. Ishihara, *Langmuir*, 2019, **35**, 1778–1787.
23 C. Yoshikawa, S. Hattori, C.-F. Huang, H. Kobayashi and M. Tanaka, *J. Mater. Chem. B*, 2021, **9**, 5794–5804.
24 M. Welch, A. Rastogi and C. Ober, *Soft Matter*, 2011, **7**, 297–302.
25 L. Li, S. Chen, J. Zheng, B. D. Ratner and S. Jiang, *J. Phys. Chem. B*, 2005, **109**, 2934–2941.
26 M. Kim, S. K. Schmitt, J. W. Choi, J. D. Krutty and P. Gopalan, *Polymers*, 2015, **7**, 1346–1378.
27 Z. Ding, C. Chen, Y. Yu and S. de Beer, *J. Mater. Chem. B*, 2022, **10**, 2430–2443.
28 J. O. Zoppe, N. C. Ataman, P. Mocny, J. Wang, J. Moraes and H. A. Klok, *Chem. Rev.*, 2017, **117**, 1105–1318.
29 S. Edmondson, V. L. Osborne and W. T. S. Huck, *Chem. Soc. Rev.*, 2004, **33**, 14–22.
30 J. Pyun, T. Kowalewski and K. Matyjaszewski, *Macromol. Rapid Commun.*, 2003, **24**, 1043–1059.
31 B. Zhao and W. J. Brittain, *Prog. Polym. Sci.*, 2000, **25**, 677–710.
32 R. Barbey, L. Lavanant, D. Paripovic, N. Schuwer, C. Sugnaux, S. Tugulu and H. Klok, *Chem. Rev.*, 2009, **109**, 5437–5527.
33 C. M. Hui, J. Pietrasik, M. Schmitt, C. Mahoney, J. Choi, M. R. Bockstaller and K. Matyjaszewski, *Chem. Mater.*, 2014, **26**, 745–762.
34 H. Klok and J. Genzer, *ACS Macro Lett.*, 2015, **4**, 636–639.
35 B. Zdyrko and I. Luzinov, *Macromol. Rapid Commun.*, 2011, **32**, 859–869.

36 R. Chiarcos, M. Perego and M. Laus, *Macromol. Chem. Phys.*, 2023, **224**, 2200400.
37 L. J. Norton, V. Smigolova, M. U. Pralle, A. Hubenko, K. H. Dai, E. J. Kramer, S. Hahn, C. Berglund and B. Dekoven, *Macromolecules*, 1995, **28**, 1999–2008.
38 P. Mansky, Y. Liu, E. Huang, T. P. Russell and C. Hawker, *Science*, 1997, **275**, 1458–1460.
39 K. S. Iyer, B. Zdyrko, H. Malz, J. Pionteck and I. Luzinov, *Macromolecules*, 2003, **36**, 6519–6526.
40 K. Viswanathan, T. E. Long and T. C. Ward, *J. Polym. Sci. Part A Polym. Chem.*, 2005, **43**, 3655–3666.
41 K. Sparnacci, D. Antonioli, V. Gianotti, M. Laus, F. F. Lupi, T. J. Giammaria, G. Seguini and M. Perego, *ACS Appl. Mater. Interfaces*, 2015, **7**, 10944–10951.
42 M. Perego, G. Seguini, E. Arduca, A. Nomellini, K. Sparnacci, D. Antonioli, V. Gianotti and M. Laus, *ACS Nano*, 2018, **12**, 178–186.
43 V. M. Ospina, R. Chiarcos, D. Antonioli, V. Gianotti, M. Laus, S. Kuschlan, C. Wiemer and M. Perego, *ACS Appl. Electron. Mater.*, 2022, **4**, 6029–6037.
44 M. Laus, R. Chiarcos, V. Gianotti, D. Antonioli, K. Sparnacci, G. Munaò, G. Milano, A. De Nicola and M. Perego, *Macromolecules*, 2021, **54**, 499–508.
45 R. Chiarcos, D. Antonioli, A. Baldanza, C. Brondi, G. Munaò, G. Milano, M. Laus and M. Perego, *Macromolecules*, 2025, **58**, 1935-1949.
46 C. Ivaldi, V. O. M. Guarin, D. Antonioli, G. Zuccheri, K. Sparnacci, V. Gianotti, M. Perego, R. Chiarcos and M. Laus, *Macromol. Rapid Commun.*, 2024, **45**, 2400288.
47 Y. Zhang, J. He, Y. Zhu, H. Chen and H. Ma, *Chem. Commun.*, 2011, **47**, 1190–1192.
48 Y. Zhu, B. Lv, P. Zhang and H. Ma, *Chem. Commun.*, 2011, **47**, 9855–9857.
49 H. A. Klok and J. Genzer, *ACS Macro Lett.*, 2015, **4**, 636–639.
50 S. Tugulu and H. Klok, *Biomacromolecules*, 2008, **9**, 906–912.
51 N. C. Ataman and H. Klok, *Macromolecules*, 2016, **49**, 9035–9047.
52 Y. Ko and J. Genzer, *Macromolecules*, 2019, **52**, 6192–6200.
53 E. D. Bain, K. Dawes, A. O. Evren, X. Hu, C. B. Gorman, J. Srogl and J. Genzer, *Macromolecules*, 2012, **45**, 3802–3815.
54 D. Paripovic and H. Klok, *Macromol. Chem. Phys.*, 2011, **212**, 950–958.
55 R. Quintana, M. Gosa, D. Jan, E. Kutnyanszky and G. J. Vancso, *Langmuir*, 2013, **29**, 10859–10867.
56 M. B. Perez, M. Cirelli and S. De Beer, *ACS Appl. Polym. Mater.*, 2020, **2**, 3039–3043.
57 F. Wang, W. Liu, R. Lu, J. Huang, B. Zuo and X. Wang, *ACS Macro*, 2022, **11**, 1041–1048.
58 P. G. de Gennes, *Macromolecules*, 1980, **13**, 1069–1075.
59 Z. Frakas, I. Derenyi and T. Vicsek, *J. Phys. Condens. Matter*, 2003, **15**, 1767–1777.
60 S. Panyukov, E. B. Zhulina, S. S. Sheiko, G. C. Randall, J. Brock and M. Rubinstein, *J. Phys. Chem. B*, 2009, **113**, 3750–3768.
61 S. S. Sheiko, S. Panyukov and M. Rubinstein, *Macromolecules*, 2011, **44**, 4520–4529.
62 L. Léger, E. Raphaël and H. Hervet, *Adv. Polym. Sci.*, 1999, **138**, 186–225.
63 J. Wang and H. Klok, *Angew. Chemie - Int. Ed.*, 2019, **58**, 9989–9993.
64 K. A. Melzak, K. Yu, D. Bo, J. N. Kizhakkedathu and J. L. Toca-herrera, *Langmuir*, 2015, **31**, 6463–6470.
65 S. Sant, K. Kaur and H. Klok, *Langmuir*, 2024, **40**, 21656–21662.
66 W. Jakubowski, K. Min and K. Matyjaszewski, *Macromolecules*, 2006, **39**, 39–45.
67 L. Michalek, L. Barner and C. Barner-Kowollik, *Adv. Mater.*, 2018, **30**, 1–18.
68 D. Antonioli, R. Chiarcos, V. Gianotti, M. Terragno, M. Laus, G. Munaò, G. Milano, A. De Nicola and M. Perego, *Polym. Chem.*, 2021, **12**, 6538–6547.
69 R. Chiarcos, D. Antonioli, V. Gianotti, M. Laus, G. Munaò, G. Milano, A. De Nicola and M. Perego, *Polym. Chem.*, 2022, **13**, 3904–3914.
70 R. Chiarcos, D. Antonioli, V. Ospina, M. Laus, M. Perego and V. Gianotti, *Analyst*, 2021, **146**, 6145–6155.

71 D. Antonioli, K. Sparnacci, M. Laus, F. Ferrarese Lupi, T. J. Giammaria, G. Seguini, M. Ceresoli, M. Perego and V. Gianotti, *Anal. Bioanal. Chem.*, 2016, **408**, 3155–3163.
72 R. Chiarcos, D. Antonioli, E. Podda, G. Muna, G. Milano, M. Perego and M. Laus, *Polymer*, 2025, **335**, 128804.
73 V. Gianotti, D. Antonioli, K. Sparnacci, M. Laus, J. T. Giammaria, M. Ceresoli, F. Ferrarese Lupi, G. Seguini and M. Perego, *J. Chromatogr. A*, 2014, **1368**, 204–210.

The data that support this work are available in the main text and in the Supporting Information.

View Article Online
DOI: 10.1039/D5PY01210D